Author Manuscript

Author Manuscript

Author Manuscript

Author Manuscript

HHS Public Access

Author manuscript

Neuron. Author manuscript; available in PMC 2018 February 08.

Published in final edited form as:

Neuron. 2017 February 08; 93(3): 616–631.e3. doi:10.1016/j.neuron.2016.12.010.

Synaptotagmin-1 and synaptotagmin-7-dependent fusion mechanisms target synaptic vesicles to kinetically distinct endocytic pathways

Ying C. Li, **Natali L. Chanaday**, **Wei Xu**, and **Ege T. Kavalali**

Department of Neuroscience, the University of Texas Southwestern Medical Center, Dallas, TX 75390-9111, USA

Summary

Synaptic vesicle recycling is essential for maintaining normal synaptic function. The coupling of exocytosis and endocytosis is assumed to be Ca^{2+}-dependent but the exact role of Ca^{2+} and its key effector synaptotagmin-1 (syt1) in regulation of endocytosis are poorly understood. Here, we probed the role of syt1 in single as well as multivesicle endocytic events using high resolution optical recordings. Our experiments showed that the slowed endocytosis phenotype previously reported after syt1 loss-of-function can also be triggered by other manipulations that promote asynchronous release such as Sr^{2+} substitution and complexin loss-of-function. The link between asynchronous release and slowed endocytosis was due to selective targeting of fused synaptic vesicles towards slow retrieval by the asynchronous release Ca^{2+} sensor synaptotagmin7. In contrast, after single synaptic vesicle fusion, syt1 acted as an essential determinant of synaptic vesicle endocytosis time course by delaying the kinetics of vesicle retrieval in response to increasing Ca^{2+} levels.

eTOC blurb

In this study, Li and colleagues demonstrate that synaptic vesicle fusion machinery comprised of synaptotagmin1, complexins and synaptotagmin7, in addition to determining the timing and Ca^{2+}-dependence of neurotransmitter release, also dictates the properties of subsequent synaptic vesicle endocytosis.

Introduction

During neuronal activity, synaptic nerve terminals release neurotransmitter via synaptic vesicle fusion with the plasma membrane in response to presynaptic action potential (AP)

Correspondence should be addressed to: Ege T. Kavalali, Department of Neuroscience, The University of Texas Southwestern Medical Center, Dallas, TX 75390-9111, Phone: 214-648-1682, Fax: 214-648-1801, Ege.Kavalali@UTSouthwestern.edu.

Author Contributions

Y.C.L., N.L.C. and E.T.K. designed the study. Y.C.L. and N.L.C. conducted the experiments and analyzed the data. W.X. contributed to the molecular experiments. Y.C.L, N.L.C. and E.T.K. (with input from W.X.) wrote the paper.

Publisher's Disclaimer: This is a PDF file of an unedited manuscript that has been accepted for publication. As a service to our customers we are providing this early version of the manuscript. The manuscript will undergo copyediting, typesetting, and review of the resulting proof before it is published in its final citable form. Please note that during the production process errors may be discovered which could affect the content, and all legal disclaimers that apply to the journal pertain.

Author Manuscript Author Manuscript Author Manuscript Author Manuscript

firing and the ensuing Ca^{2+} influx. However, the endocytic pathways that retrieve synaptic vesicles after fusion are poorly understood (Kononenko and Haucke, 2015). The coupling of exo- and endocytosis is assumed to be Ca^{2+} dependent but the mechanism is still unknown (Wu et al., 2014). Importantly, key questions on the exact role of Ca^{2+} and its effectors in regulation of endocytosis remain open as experiments assessing the impact of Ca^{2+} on synaptic vesicle retrieval provided wide ranging and often conflicting results (Leitz and Kavalali, 2015). Under certain conditions and preparations, Ca^{2+} has been shown to slow endocytic retrieval (von Gersdorff and Matthews, 1994; Leitz and Kavalali, 2011), in others, Ca^{2+} has been demonstrated to have a positive effect, facilitating synaptic vesicle retrieval (Marks and McMahon, 1998; Sankaranarayanan and Ryan, 2000; Wu et al., 2009). At the single synaptic vesicle level, Ca^{2+} has been shown to slow retrieval in a manner that is not shared by synaptic vesicles that fuse spontaneously (Leitz and Kavalali, 2014). These seemingly conflicting observations contrast with our more in-depth and precise understanding of the key molecular players that give rise to synaptic vesicle exocytosis (Sudhof, 2013). Nevertheless, it is well-established that the fidelity of synaptic transmission and the structural homeostasis of nerve terminals rely on the efficient recycling of synaptic vesicles after neurotransmitter release (Kavalali, 2006).

Synaptic vesicle protein synaptotagmin-1 (syt1) acts as a key Ca^{2+} sensor for fast synchronous synaptic vesicle exocytosis but it is also implicated in synaptic vesicle endocytosis (Geppert et al., 1994, Fernandez-Chacon et al., 2001, Sudhof 2004; Sudhof, 2013). Early biochemical experiments have demonstrated that syt1 interacts with clathrin adaptor protein (AP-2) suggesting a role in clathrin-mediated endocytosis and coupling synaptic vesicle fusion to retrieval (Zhang et al., 1994; Haucke and De Camilli, 1999; von Poser et al., 2000). Accordingly, experiments with constitutive syt1 knockout (syt1 KO) neurons revealed slower endocytosis rate compared to wild type (WT) neurons (Nicholson-Tomishima and Ryan, 2004). In the *Drosophila* neuromuscular junction acute inactivation of syt1 function also gave rise to impaired synaptic vesicle endocytosis (Poskanzer et al., 2003). In adrenal chromaffin cells, endocytosis has been shown to switch from being Ca^{2+}-dependent to Ca^{2+}-independent in the absence of syt1 (Yao et al., 2012a). Site-directed mutagenesis experiments in the Ca^{2+} binding domains (C2A and C2B) of syt1 suggest that the Ca^{2+} sensing role of syt1 is critical not only for exocytosis, but also for endocytosis (Poskanzer et al., 2006; Yao et al., 2012b). Mutations of the Ca^{2+} binding residues in the C2B domain of syt1 slow endocytosis rates to the same level as in syt1-null *Drosophila* neuromuscular junctions (Poskanzer et al., 2006). Similar syt1 mutants that inhibited the Ca^{2+} binding function of C2A or C2B also failed to rescue rapid endocytosis in syt1 KO mouse neurons (Yao et al., 2012b).

A major challenge in studying the function of syt1 in endocytosis is separating its role in exocytosis from its putative involvement in synaptic vesicle retrieval. Most studies to date have relied on strong stimulation to evaluate synaptic vesicle retrieval after multi-vesicular exocytosis (Leitz and Kavalali, 2015). This work, therefore, has been unable to reconcile previously observed differences in the role of Ca^{2+} in synaptic vesicle endocytosis with syt1 function. In particular, it is plausible to expect that syt1's role in endocytosis may diverge after exocytosis of single vesicles versus vesicle retrieval following tandem release of multiple vesicles in rapid succession. Here, we examined single vesicle versus multi-vesicle

Author Manuscript Author Manuscript Author Manuscript Author Manuscript

endocytic events using the improved signal-to-noise characteristics of vGlut1-pHluorin in syt1-deficient neurons to further probe syt1's role in Ca^{2+}-dependent synaptic vesicle recycling. Our results demonstrated that syt1 along with other key synaptic vesicle fusion machinery components (i.e. complexins and synaptotagmin7) determine the rate of synaptic vesicle endocytosis during repetitive activity. In contrast, after single synaptic vesicle fusion, syt1 acts as a key determinant of synaptic vesicle endocytosis time course in response to alterations in Ca^{2+} levels.

Results

Syt1-knock down in hippocampal neurons slows multivesicle retrieval after repetitive stimulation

To investigate the role of syt1 in synaptic vesicle endocytosis, we used a previously characterized shRNA knock down (KD) construct to suppress syt1 expression in rat hippocampal neurons (Xu et al., 2012) (Figure 1A). Under these conditions, using whole cell voltage clamp recordings, we detected a decrease in peak evoked inhibitory postsynaptic current (IPSC) amplitudes in combination with an increase in asynchronous release compared to wild type (WT) neurons (Figure 1B–D). Both phenotypes could be rescued by co-expression of a shRNA resistant syt1 construct indicating that they were specific to syt1 loss-of-function (Figure 1B–D). Moreover, under the same conditions, we observed an increase in the frequency of spontaneous miniature IPSCs (mIPSCs), which could also be reduced back to WT levels after co-expression of the same shRNA resistant syt1 construct (Figure S1 A–C). These findings indicate that acute KD of syt1 expression completely recapitulates the neurotransmitter release phenotypes previously reported in syt1 KO neurons (Maximov and Sudhof, 2005) and thus validate the use of syt1 shRNA KD construct to further explore synaptic vesicle trafficking.

To monitor the properties of synaptic vesicle retrieval, we infected hippocampal neurons with a lentivirus expressing a well-characterized probe where a pH-sensitive GFP is attached to the vesicle lumen region of vesicular glutamate transporter-1 (vGlut1-pHluorin) (Voglmaier et al., 2006), which shows low levels of surface expression and substantially improved signal-to-noise ratio compared to other similar probes (Kavalali and Jorgensen, 2014) (Figure 1E). When we stimulated vGlut1-pHluorin expressing neurons with 100 APs at 20 Hz, we detected significantly slower decay of fluorescence back to baseline levels after syt1 KD (Figure 1F–G). This is consistent with a slowed multivesicular endocytosis rate, since the endocytic time course largely outlasts asynchronous release time course (decay time constants of ~50 s and ~0.5 s, respectively, compare figure 1B and D to 1F and G). Again, this finding also replicates the slowed endocytosis phenotype previously observed in syt1 KO neurons (Nicholson-Tomishima and Ryan, 2004).

Syt1 loss-of-function accelerates single synaptic vesicle endocytosis

Next, we aimed to detect single synaptic vesicle retrieval taking advantage of the improved signal-to-noise ratio characteristics of vGlut1-pHluorin (Balaji and Ryan, 2007) based on the methodology previously described by our laboratory (Leitz and Kavalali, 2011). For this purpose, we triggered synaptic vesicle fusion at low frequency and detected positive

Author Manuscript Author Manuscript Author Manuscript Author Manuscript

fluorescence fluctuations with amplitudes two standard deviations above the mean baseline noise (Figure 1H). In the presence of 2 mM Ca^{2+} in the extracellular medium, each positive fluorescence fluctuation was followed by swift decay back to baseline fluorescence consistent with rapid vesicle retrieval and re-acidification (Figure 1H inset). The amplitudes of these evoked fusion events were comparable to the spontaneous fusion events we detected under the same conditions (albeit in the presence of the Na^{+} channel blocker TTX) corroborating their single vesicle origin (Figure S1 D–E) (also see Leitz and Kavalali, 2014). This setting allowed us to systematically investigate Ca^{2+}-dependence of neurotransmitter release probability (Pr) by counting events at each stimulation as failures (events within two standard deviations of baseline noise) or successes (two standard deviations above the mean baseline noise) (Figure 1H inset). We then calculated the Pr as the ratio of successful events to the total number of stimuli (i.e. trials) applied to a given synapse. Under these conditions we detected single evoked fusion events with a median probability of 0.1 (Figure 1H, also see Leitz and Kavalali, 2011) indicating that these settings enable visualization of release from single synapses (Murthy et al., 1997). However, knockdown of syt1 resulted in a dramatic decrease in Pr by increasing the propensity of failures (Figure 1I). Syt-1 loss-of-function also suppressed the Ca^{2+}-dependent increase in Pr as rightward shifts seen in Pr distributions at 4 and 8 mM Ca^{2+} (Figure 1I–L). These results agree well with earlier findings on the key role of syt1 in Ca^{2+}-dependent regulation of evoked Pr (Fernandez-Chacon et al., 2001). Moreover, under the same conditions we detected a substantial decrease in the prevalence of high amplitude events seen in elevated extracellular Ca^{2+} concentrations that may reflect multivesicular fusion (Leitz and Kavalali, 2011) (Figure S1 F–H). This result indicates that syt1 loss-of-function does not only impair Ca^{2+}-dependent increase in Pr but also diminishes multivesicular release.

Analyzing single-vesicle retrieval kinetics in syt1 KD neurons also revealed a previously unknown function of syt1. In earlier work, we have observed a profound increase in the dwell times of evoked single vesicle fusion events in response to increasing Ca^{2+} levels (Leitz and Kavalali, 2011). Dwell time reports the residency of vGlut1-pHluorin molecules at the presynaptic plasma membrane prior to retrieval and ranges between <1s at 2 mM Ca^{2+} up to 20s at 8 mM Ca^{2+} (Figure 2A–F). Perfusion of a weak acid buffer (pH~6.6) can completely extinguish these dwell times even at high Ca^{2+} concentrations, while still allowing to detection of rapid fusion events, thus supporting the premise that these fluorescence dwell times indeed represent residency of vGlut1-pHluorin probes at the surface membrane before retrieval (Figure 2G). The substantive increase in surface residency seen at elevated Ca^{2+} concentrations only follows evoked fusion but does not happen during spontaneous synaptic vesicle retrieval (Leitz and Kavalali, 2014). Interestingly, following syt1 loss-of-function, we did not detect this increase in the duration of single vesicle dwell times despite the robust Ca^{2+}-dependent increase in the same parameter in control neurons (Figure 2A–F). Importantly, syt1 KD's negative effect on single vesicle dwell times was also evident at 2 mM Ca^{2+} indicating a key role for syt1 in regulating the residency of synaptic vesicle proteins at the surface membrane after fusion (Figure 2H–J). Since only unitary quantal fluorescence amplitudes were selected for analysis (based on the information presented in figure S1), and average dwell time duration was ~10 fold (at 2 mM Ca^{2+}) and ~50 fold (at 8 mM Ca^{2+}) longer than the mean decay time constant of IPCSs in the same

Author Manuscript Author Manuscript Author Manuscript Author Manuscript

conditions (Figure S2A–B), these two observations argue that Ca^{2+}-dependent prolongation in fluorescence dwell times in control neurons is not a consequence of the fusion of multiple vesicles either synchronously or asynchronously, respectively. Furthermore, decay time constants of single action potential IPSCs were ~2 fold higher in syt1 KD neurons compared to control and increased with extracellular Ca^{2+} concentration in both groups (figure S2A) even though we observed the opposite trend in single vesicle endocytosis events, i.e. in syt1 KD neurons endocytosis occurs significantly faster and is Ca^{2+}-independent (compare figure S2 A to B). Taken together these results point towards a role for syt1 in delaying endocytosis after single vesicle fusion. The impact of syt1 KD on Ca^{2+}-dependent regulation of single vesicle dwell times also extended to the fluorescence decay time courses of single vesicle events that are thought to reflect the re-acidification time course of vesicles after retrieval (Figure S2 C–H). Here it is important to note that, this dramatic effect of syt1 KD on single vesicle retrieval kinetics was indeed specific to syt1 function as it could be rescued by co-expression of a shRNA-resistant syt1 (see Figure 7 below).

Sr^{2+} substitution promotes asynchronous release and slows endocytosis after repetitive activity

Our experiments so far suggest that syt1 has two seemingly opposite functions in the regulation of synaptic vesicle endocytosis. In response to repetitive stimulation, as reported previously, syt1 appears to facilitate synaptic vesicle retrieval, whereas following single vesicle fusion it delays vesicle retrieval in a Ca^{2+}-dependent manner. To resolve this dichotomy we aimed to create a condition where asynchronous release is elevated mimicking the phenotype of syt1 loss-of-function by substituting Sr^{2+} for Ca^{2+}. Sr^{2+} has been widely used as a tool to promote asynchronous release (Dodge et al., 1969), a property that arises from its slower clearance from presynaptic terminals compared to Ca^{2+} (Xu-Friedman and Regehr, 2000) as well as its differential affinity for Ca^{2+} sensors such as syt1 (Shin et al., 2003; Evans et al., 2015). In whole cell voltage-clamp recordings, substituting Sr^{2+} for Ca^{2+} resulted in substantial desynchronization of release where neurotransmitter release events returned to their baseline levels with a longer delay after application of 100 APs at 20 Hz (Figure 3A–C). Under the same conditions, in optical experiments we detected slower endocytosis after 20 Hz stimulation in a manner similar to our observations after syt1 KD (Figure 3D–E). Thus, after stimulation that releases multiple synaptic vesicles, substitution of Ca^{2+} with Sr^{2+} slows endocytosis and recapitulates the effects of syt1 KD. In agreement with this premise, Sr^{2+} substitution failed to further decrease fluorescence decay times in syt1 KD neurons, consistent with the occlusion of the Sr^{2+} effect in the absence of syt1 (Figure 3D–E).

Sr^{2+} substitution slows single vesicle retrieval in the same manner as Ca^{2+}

Although substituting Sr^{2+} for Ca^{2+} mimicked the repetitive stimulation-driven slowed endocytosis phenotype syt1 KD, Sr^{2+} substitution did not recapitulate syt1 KD at the single-vesicle level (Figure 4A–C). Fusion events evoked by sparse low frequency stimulation (0.01–0.2 Hz) responded to increasing Sr^{2+} concentrations in the same fashion observed for Ca^{2+}, i.e. prolonging single vesicle retrieval kinetics (Figure 4D–F and Figure S3). Moreover, this slowdown in single vesicle retrieval kinetics, as in the case of Ca^{2+}, strictly depended on syt1 expression since it was absent in syt1 KD neurons (Figure 4G–I). This

Author Manuscript Author Manuscript Author Manuscript Author Manuscript

result demonstrates that both Ca^{2+} and Sr^{2+} interact with syt1 to delay single synaptic vesicle retrieval. However, after repetitive stimulation Sr^{2+} substitution simply mimics syt1 loss-of-function. As indicated above, both syt1 loss-of-function and Sr^{2+} substitution desynchronizes neurotransmitter release especially during repetitive stimulation. Therefore, the Sr^{2+} mediated uncoupling of the mechanisms of endocytosis after repetitive stimulation versus single vesicle retrieval may indicate that asynchronously released vesicles are preferentially targeted to a slower endocytic pathway. To test this premise, in the next set of experiments, we investigated the impact of alternative means to desynchronize neurotransmission and promote asynchronous release on subsequent endocytosis.

Knock down of complexin 1/2 slows endocytosis after repetitive stimulation

Complexins (cpx) comprise a family of small proteins that bind to soluble N-ethylmaleimide-sensitive factor attachment protein receptor (SNARE) complexes (McMahon et al., 1995; Tang et al., 2006) and as such they promote synaptic vesicle priming for fusion and cooperate with syt1 in Ca^{2+} triggering of fusion (Reim et al., 2001; Maximov et al., 2009). Loss-of-function of cpx-1 and -2 — the most abundant cpx subtypes in the CNS — in hippocampal neurons results in an impairment in synchronous release (Reim et al., 2001) and an increase in asynchronous release (Maximov et al., 2009). To evaluate the impact of cpx loss-of-function on synaptic vesicle endocytosis, we used previously characterized shRNA constructs that elicit KD of both cpx1 and cpx2 (Maximov et al., 2009; Yang et al., 2013). In agreement with earlier work, whole cell voltage clamp recordings from neurons infected with the cpx1/2 KD construct revealed enhancement of asynchronous release after 100AP-20Hz stimulation (Figure 5A–C) (Maximov et al., 2009). Under the same conditions, optical recordings revealed a dramatic slowdown in fluorescence decay time course after repetitive stimulation, even greater than what we observed in syt1 KD, indicating a decrease in the rate of synaptic vesicle retrieval (Figure 5D–E). Nevertheless, the effects of cpx1/2 KD and syt1 KD were not additive, since double KD (DKD) neurons only showed a small, non-significant, increase in decay τ compared to cpx1/2 KD, supporting their cooperative action at synaptic vesicle retrieval (Figure 5D–E). In contrast, when we examined the impact of cpx loss-of-function on single vesicle retrieval, we detected an increase in single vesicle retrieval time course in response to elevated Ca^{2+} concentrations as in control neurons (Figure 5F–G), although in cumulative histograms of single vesicle dwell times, synapses deficient in cpx compared to control synapses showed a slightly reduced ability to respond to elevated Ca^{2+} (Figure 5H–I). Interestingly, the difference between cpx1/2 KD synapses and controls were more pronounced when single vesicle decay time constants —reporting vesicle re-acidification—were compared (Figure S4). Therefore, cpx loss-of-function effect on the kinetics of individual events may partly mimic syt1 loss-of-function as complexin may also alter factors regulating vesicle re-acidification (e.g. vesicle size, v-ATPase function). Furthermore, under mild stimulation, cpx1/2 and syt1 DKD neurons showed the same phenotype as syt1 KD, with fast and Ca^{2+}-independent single vesicle retrieval, supporting that complexin loss-of-function does not exacerbate syt1 deficiency in single vesicle endocytosis (Figure 5I and S4D).

Taken together, our results so far suggest a strong link between the mechanism of fusion and the kinetics of subsequent endocytosis. Vesicles released asynchronously (or in a

Author Manuscript Author Manuscript Author Manuscript Author Manuscript

desynchronized manner) during repetitive stimulation after syt1 loss-of-function, Sr^{2+} substitution or cpx loss-of-function are retrieved far slower with a time course that outlasts the delayed fusion kinetics of asynchronous release. At the single vesicle fusion level, however, Ca^{2+} and Sr^{2+} elevation could prolong retrieval in a manner that strictly required syt1 but did not show substantial dependence on complexin expression suggesting a key role for syt1 in regulation of single synaptic vesicle retrieval kinetics. If this Ca^{2+}-dependent slowdown in single synaptic vesicle retrieval kinetics reflects a highly specific function of syt1, then how can one reconcile this effect with syt1's apparent ability to facilitate endocytosis after repetitive stimulation? To address this puzzle, in the next set of experiments, we investigated the role of synaptotagmin7 (syt7) which is an alternative Ca^{2+} sensor that binds Ca^{2+} with higher affinity (Sugita et al., 2002) in the regulation of endocytosis.

Synaptotagmin7 supports asynchronous release and slows vesicle retrieval during repetitive activity

Syt7 has recently emerged as a key Ca^{2+}-sensing synaptic protein that maintains asynchronous neurotransmitter release independently of syt1 (Wen et al., 2010; Bacaj et al., 2013, Jackman et al., 2016). In addition, earlier work from our group has shown that the full-length splice variant of syt7 that retains both C2-domains decelerates recycling and preferentially targets synaptic vesicles to a slow recycling pathway (Virmani et al., 2003). To test the premise that syt7 may play a role in controlling vesicle retrieval after repetitive stimulation mediated asynchronous release, we suppressed the levels of syt7 expression along with syt1 KD (Figure 6A). In electrophysiological experiments, we detected a substantial reduction in asynchronous release in syt1/syt7 DKD neurons (compared to syt1 loss-of-function), replicating earlier findings (Figure 6B–C) (Bacaj et al., 2013). Importantly, under the same conditions after syt1 loss-of-function, optical experiments revealed a marked facilitation of endocytic retrieval following syt7 KD (Figure 6D–E) apparently rescuing the impact of syt1 deficiency on vesicle retrieval. Conversely, syt7 overexpression (OE) slowed endocytosis compared to controls (Figure 6F–G) corroborating our earlier findings that syt7 indeed has a bona fide role in slowing endocytic retrieval during activity (Virmani et al., 2003). However, syt7 OE on syt1 KD neurons did not lead to a further increase in fluorescence decay τ, supporting the premise that both manipulations are affecting the same pathway (Figure 6F–G). In parallel experiments, we found that expression of a truncated syt7 (syt7 T) splice variant that lacks both C2 domains also slowed down the retrieval of multiple fused vesicles to the same extent as full length syt7 OE (Figure 6G). This result implies that syt7 C2 domains are dispensable for the form of endocytic regulation we observed. Interestingly, syt7 KD alone did not appear to significantly alter endocytosis compared to controls, agreeing with the previous report of normal synchronous IPSC responses in synapses lacking syt7 (Maximov et al., 2008). Nevertheless, syt7's role in delaying release becomes relevant under strong, repetitive stimulation and particularly in synapses that encode information through prolonged, asynchronous release of neurotransmitter (Luo et al., 2015) suggesting that in WT hippocampal neurons syt1 has a dominant role in the regulation of not only fast release but also the kinetics of endocytosis (Figure 6D–E). In agreement with this premise, syt7 KD or syt7 OE did not significantly alter the rate of single synaptic vesicle retrieval during sparse

Author Manuscript Author Manuscript Author Manuscript Author Manuscript

stimulation (Figure 6H–I). This result bolsters the notion that Ca^{2+}-dependent regulation of single synaptic vesicle endocytosis is a genuine function of syt1, whereas multivesicular retrieval after repetitive stimulation may depend on multiple factors besides syt1 such as complexins and syt7.

The impact of syt1 Ca^{2+}-binding and membrane penetration properties in single-vesicle retrieval

To investigate the putative mechanisms underlying syt1's role in Ca^{2+}-dependent regulation of single vesicle retrieval, we assessed the importance of Ca^{2+}-binding and membrane penetration properties for syt1 function. Synchronicity of release is supported by a cooperative binding of Ca^{2+} to both syt1 C2 domains, which in turn rapidly increases its affinity for negatively charged phospholipids and the SNARE complex (Sudhof, 2012). However, C2A and C2B domains have been reported to be dissimilar in terms of their Ca^{2+} affinity and protein interactions, thus differentially impacting syt1 function (Rizo and Rosenmund, 2008). To evaluate Ca^{2+}-binding and membrane penetration properties for syt1 in regulation of single-vesicle retrieval we analyzed the rescuing capacity of different mutants at 8 mM extracellular Ca^{2+} in order to fully uncover differences amongst groups and the effects of the mutations. We first studied the effect of eliminating Ca^{2+}-binding by mutating two Ca^{2+}-interacting amino acids on each C2 domain or both (see Figure 7A for details). Lentiviral infection with syt1 mutated on its C2A domain (C2A*) or in both domains (C2A*/C2B*) failed to rescue syt1 KD phenotype at the single-vesicle level (Figure 7C and F, and S5 A and D). Interestingly, expression of syt1 with a C2B domain incapable of binding to Ca^{2+} (C2B*) could partially rescue syt1 KD single-vesicle retrieval dwell times and decay τ (Figure 7B and E, and S5 A and D). Indicating that Ca^{2+}-binding to syt1 C2A domain has a stronger contribution to regulating single-vesicle endocytosis, although Ca^{2+}-binding to both domains are necessary to reach a full rescue (compare Figure 7D and E). These results were not due to alterations in the sequence or the expression levels of the mutant proteins in our hands, since for strong stimulation we replicated previous findings (i.e. syt1 C2A* mutant could rescue amplitude and decay τ, while syt1 C2B* mutant could not, data not shown and see (Yao et al., 2012a)). We then studied the effect of manipulating syt1 membrane penetration ability. Lentiviral expression of a syt1 mutant that is able to bind SNAREs and Ca^{2+} but unable to penetrate membranes (syt1 4A, see (Yao et al., 2012a)) could not rescue syt1 KD, demonstrating that phospholipid interaction is essential for syt1's role in single-vesicle retrieval (Figure 7C and F, and S5 B and E). In agreement with this premise, a mutation that enhances syt1 membrane binding in response to Ca^{2+} (syt1 4W, and (Yao et al., 2012a)) could significantly rescue dwell times and decay τ, although not to the same extent as full length syt1 (Figure 7C, D and F, and S5 B, C and E). Taken together, these results indicate that coordination of Ca^{2+} binding and phospholipid interactions are required for syt1 mediated regulation of single-vesicle endocytosis.

Properties of syt7 trafficking during neuronal activity

So far our results support a model where, under strong stimulation, syt7 has a privileged role in directing synaptic vesicles to a slow endocytic pathway, whereas syt1 acts as specific controller of vesicle retrieval under mild, single AP stimulation. In contrast to syt1's specific localization to synaptic vesicles, syt7 was previously reported to be more concentrated on

Author Manuscript Author Manuscript Author Manuscript Author Manuscript

the presynaptic plasma membrane or other internal membranes, but not synaptic vesicles (Takamori et al., 2006; Virmani et al., 2003). Overexpression of syt7 in hippocampal neurons also leads to a slower synaptic vesicle recycling pathway triggering emergence of large membranous structures (Virmani et al., 2003). To examine syt7 trafficking we generated a fusion protein between syt7 and the pH sensitive GFP (syt7-pHluorin, Figure 8A). Syt7-pHluorin distribution resembled the previously reported one for wild type syt7 (Virmani et al., 2003), where 40–80 % of syt7 was present on the surface membrane and between 20–60 % was present intracellularly (Figure 8B). Mild electrical stimulation at 1 Hz did not generate detectable changes in syt7-pHluorin signals (Figure 8 C–D) indicating that syt7 is not engaged in recycling under mild stimulation (in contrast to substantial trafficking of vGlut1-pHluorin under the same conditions, see Leitz and Kavalali, 2011). However, syt7-pHluorin was robustly endocytosed in response to 20 Hz stimulation (Figure 8E–G) and increasing the number of stimuli and extracellular Ca^{2+} concentration led to subsequent recycling of syt7-pHluorin back to the membrane (see the shift towards positive ΔF_{max} values in Figure 8E–G). In additional experiments perfusion of 90 mM KCl caused a substantial increase in fluorescence as reported earlier (data not shown) (Dean et al., 2012) indicating that syt7 recycling is dependent on the strength and previous history of stimulation. This result provides insight into syt7's unique ability to influence vesicle recycling during strong stimulation by demonstrating that syt7 undergoes a completely different recycling pathway than syt1, and syt7 participation in recycling is only detectable under strong, repetitive activity.

Discussion

Synaptic vesicle retrieval after asynchronous release

In this study, our results demonstrated that the synaptic vesicle fusion machinery comprised of syt1, complexins as well as syt7, while dictating the timing and Ca^{2+}-dependence of neurotransmitter release, also exerts a strong influence on the properties of synaptic vesicle endocytosis. Our optical experiments — based on monitoring the trafficking of vGlut-1-pHluorin tagged synaptic vesicles — replicated earlier findings and demonstrated that after repetitive stimulation syt1 facilitates the pace of synaptic vesicle retrieval (Poskanzer et al., 2003; Balaji and Ryan, 2007; Yao et al., 2012b). However, our additional experiments showed that the same "slowed endocytosis" phenotype can also be triggered by Sr^{2+} substitution as well as cpx loss-of-function, all manipulations that promote asynchronous release, thus suggesting a link between desynchronization of neurotransmitter release and the subsequent rate of synaptic vesicle retrieval. This putative link between asynchronous release and slowed endocytosis was supported by the subsequent experiments demonstrating the role of the asynchronous release Ca^{2+} sensor syt7 in endocytosis. These experiments revealed that the slowed vesicle retrieval seen after repetitive stimulation is influenced by syt7 as syt7 knockdown resulted in rescue of fast endocytosis impaired after syt1 loss-of-function. In agreement with this observation, syt7 overexpression substantially slowed endocytosis consistent with the earlier proposal that syt7 selectively targets synaptic vesicles to a slow endocytic pathway (von Poser et al. 2000; Virmani et al., 2003). At the ultrastructural level, the syt7-dependent reduction in endocytosis kinetics was also associated with preferential retrieval of large endocytic structures after strong stimulation

Author Manuscript Author Manuscript Author Manuscript Author Manuscript

(Virmani et al., 2003). This premise is consistent with syt7's predominant localization on the presynaptic plasma membrane — in contrast to syt1's specific localization to synaptic vesicles (Takamori et al., 2006; Virmani et al., 2003). Accordingly, syt1 and syt7 show vastly different trafficking trajectories. While syt1-pHluorin was previously shown to label the same vesicle pool and recycled in the same way as vGlut1-pHluorin (Fernandez-Alfonso and Ryan, 2008), syt7-pHluorin was refractory to stimulation (Dean et al., 2012). Here we show that the same strong stimulation used to elicit asynchronous release and slow endocytosis can trigger syt7 endocytosis and subsequently syt7 is capable of being recycled back to the presynaptic plasma membrane. Thus syt7 likely performs its role at the plasma membrane and recruits the molecular machinery triggering the slow mode of endocytosis (Weber et al., 2014). Strikingly, expression of a short splice variant of syt7 lacking both C2 domains (syt7 T) had the same effect on vesicle retrieval kinetics as full length syt7, indicating that Ca^{2+}-binding is not essential for syt7's function in dampening the rate of endocytosis.

Taken together, these results highlight the key role of the Ca^{2+}-dependent fusion machinery in dictating the subsequent kinetics and pathway of synaptic vesicle endocytosis where asynchronously released vesicles are selectively targeted to a slower synaptic vesicle trafficking pathway compared to their synchronously released counterparts.

Mechanisms underlying the kinetics of single synaptic vesicle retrieval

In contrast to the experiments conducted using repetitive stimulation, single synaptic vesicle retrieval kinetics assessed using sparse low frequency stimulation remained unaffected by syt7 gain- or loss-of-function. In these experiments, properties of single synaptic vesicle retrieval strictly depended on syt1 expression and was relatively unaffected by complexin loss-of-function. Moreover, substituting Sr^{2+} for Ca^{2+} did not result in a significant alteration of single vesicle retrieval properties nor their dependence on syt1.

What is the syt1-mediated mechanism that underlies the Ca^{2+}-dependent prolongation of single synaptic vesicle retrieval? Our results may provide the following clues into this question. The time course of delayed single vesicle retrieval far outlasted the time course of action potential evoked presynaptic Ca^{2+} transients (Figures S6A–C). Therefore, they are likely mediated by increases in baseline Ca^{2+} seen under these conditions (Figure S6D–F), consistent with the previously reported EGTA-AM sensitivity of this phenomenon (Leitz and Kavalali, 2011). In elevated baseline Ca^{2+} conditions, syt1 may continue its engagement with its effectors after fusion thus slowing vesicle retrieval. Accordingly, we found that a syt1 mutant incapable of binding Ca^{2+} in both C2 domains lost its ability to rescue Ca^{2+}-dependent delay in single vesicle endocytosis. Interestingly, for single vesicle retrieval Ca^{2+}-binding to the C2A domain seems to be more important than to C2B, in contrast to what was described for syt1's role in synchronous neurotransmitter release (Rizo and Rosenmund, 2008). At the drosophila neuromuscular junction, a syt1 mutant carrying two C2B domains, and no C2A, can rescue normal synaptic vesicle docking on syt1 KO terminals, but it fails to rescue altered vesicle size and number, consistent with the notion that the presence of a C2A domain is required for syt1's regulation of vesicle retrieval and recycling (Lee et al., 2013). The effectors through which syt1 exerts its role may either consist of the SNARE complex or

Author Manuscript Author Manuscript Author Manuscript Author Manuscript

membrane lipids (Sudhof, 2013). The preservation of endocytic kinetics after Sr^{2+} substitution implies that syt1-lipid interactions rather than syt1's engagement with the SNARE complex may determine the time course of single vesicle retrieval as Sr^{2+} — unlike Ca^{2+}— has been shown to be a poor mediator of syt1-SNARE complex interactions (Shin et al., 2003). In agreement with this premise, our experiments showed that besides Ca^{2+}-binding, membrane penetration is needed for syt1's modulation of single vesicle endocytosis, since a membrane penetration deficient mutant (syt1 4A) was unable to rescue the phenotype while syt1 with increased membrane affinity (syt1 4W) could significantly rescue the kinetics and Ca^{2+} sensitivity of single vesicle retrieval. In conclusion, our results suggest a mechanism where syt1 delays single vesicle retrieval via its prolonged interactions with the presynaptic plasma membrane in a Ca^{2+}-regulated manner.

Direct impact of the fusion machinery on the properties of synaptic vesicle retrieval

Taken together, our findings reveal the strong impact of the fusion machinery in dictating the properties of synaptic vesicle retrieval. This premise agrees well with earlier work from our group as well as others which demonstrated the essential role of the vesicular SNARE protein synaptobrevin2 (also called VAMP2) in rapid synaptic vesicle retrieval (Deak et al., 2004; Hosoi et al., 2009; Xu et al., 2013). The impact of synaptobrevin2 on vesicle retrieval may also be shared with the function of target membrane SNARE SNAP-25 in endocytosis (Xu et al., 2013, but see Bronk et al., 2007). Slowed kinetics of endocytic retrieval seen after synaptobrevin2 and SNAP-25 loss-of-function is consistent with the current observation that synapses deficient in SNARE complex binding proteins complexin 1 and 2 also manifest slow endocytosis after repetitive stimulation. These findings indicate that compromising rapid canonical SNARE-mediated fusion machinery — including SNAREs, complexins and syt1— targets synaptic vesicles to an alternative slow endocytic pathway that relies at least in part on syt7.

The mechanisms that underlie this syt7-driven coupling of asynchronous release to a slow endocytic pathway, however, remain poorly understood. In earlier work, our group has demonstrated that the alternative vesicular SNARE protein VAMP4 can be selectively recruited to synaptic vesicles endocytosed after strong stimulation (Raingo et al., 2012). In the current study, we found that syt7-pHluorin trafficking follows a trajectory very similar to the one we previously described for VAMP4-pHluorin. Interestingly, VAMP4 has recently been shown to be a specific mediator of activity-dependent bulk endocytosis, which is a non-canonical endocytic pathway activated during strong stimulation (Nicholson-Fish et al., 2015). When viewed together with our current findings, these earlier results suggest that impairing the classically defined rapid synaptic fusion machinery or delivering strong stimulation to augment asynchronous neurotransmitter release may target synaptic vesicles to these alternative recycling pathways governed by distinct endocytic mediators such as VAMP4 and/or syt7 (Figure 8H). These mechanisms may help diversify the molecular compositions of synaptic vesicles regenerated after fusion and provide presynaptic terminals with a wide range of synaptic vesicle populations with distinct biogenesis properties, fusion propensities. This diversity may in turn help presynaptic terminals respond to extrinsic factors and stimuli selectively to promote specific forms of neurotransmission with dedicated signaling roles (Bal et al., 2013).

Author Manuscript Author Manuscript Author Manuscript Author Manuscript

STAR METHODS

CONTACT FOR REAGENT AND RESOURCE SHARING

Lead Contact: Ege T. Kavalali, Department of Neuroscience, The University of Texas Southwestern Medical Center, Dallas, TX 75390-9111. Phone: 214-648-1682 E-mail: Ege.Kavalali@UTSouthwestern.edu

The Lead Contact (ETK) holds responsibility for responding to requests and providing reagents and information.

EXPERIMENTAL MODEL AND SUBJECT DETAILS

Dissociated hippocampal cultures—Both hippocampi were dissected from postnatal day 2–4 Sprague-Dawley rats and subsequently neurons were dissociated using 10 mg/ml trypsin (10 min at 37°C) and triturated with a P1000 pipette. Cell suspensions were plated onto 12 mm coverslips coated with Matrigel in a concentration of two hippocampi per 10–12 coverslips. Basic growth medium consisted of MEM medium (no phenol red), 5g/l D-glucose, 0.2g/l $NaHCO_3$, 100mg/l transferrin, 5% of heat inactivated fetal bovine serum, 0.5 mM L-glutamine, 2% B-27 supplement, and 2–4 μM cytosine arabinoside. Cultures were kept in humidified incubators at 37°C and gassed with 95% air and 5% CO_2.

METHOD DETAILS

Lentiviral infection of hippocampal cultures—The vGlut1-pHluorin construct was a gift from Drs. R.H. Edwards and S.M. Voglmaier (University of California, San Francisco) (Voglmaier et al., 2006). Constructs expressing syt1 membrane penetration mutants and Ca^{2+} binding mutants were provided by Dr. Edwin Chapman (University of Wisconsin, Wisconsin) (Yao et al., 2012a). All lentiviral knockdown and rescue constructs used were gifts from Dr. T.C. Südhof (Stanford University) and have been previously validated (Maximov et al., 2009; Xu et al., 2012; Bacaj et al., 2013). Lentiviruses were produced in HEK293 cells (ATCC) by contransfection of pFUGW/L307 transfer vectors and 3 packaging plasmids (pCMV-VSV-G, pMDLg/pRRE, pRSV-Rev) using Fugene 6 transfection reagent (Promega). Cell culture supernatants containing the viruses were harvested 48 hours after transfection and clarified by low speed centrifugation for infection of neurons at 4 DIV. All experiments were performed on 14–21 DIV cultures when synapses were mature and lentiviral expression of constructs of interest was optimal (Mozhayeva et al., 2002; Deak et al., 2006). All experiments were performed following protocols approved by the UT Southwestern Institutional Animal Care and Use Committee.

Western blotting—Neuronal cultures were harvested using Laemmli sample buffer and subjected to SDS-PAGE followed by Western blot to assess knockdown efficacy of syt1, cpx1/2, syt7. Primary antibodies anti-syt1 mouse monoclonal, anti-syt7 rabbit polyclonal, anti-cpx1/2 rabbit polyclonal, anti-GDI mouse monoclonal and anti-syb2 mouse monoclonal were used at 1:1000 dilution (Synaptic Systems). Immunoreactive bands were visualized by enhanced chemiluminescence (ECL), captured on autoradiography film and analyzed using ImageJ software. Syt1, cpx1/2 and syt7 protein levels were normalized to syb2 loading control.

Author Manuscript Author Manuscript Author Manuscript Author Manuscript

Electrophysiology—Cultured pyramidal neurons were used between 14 to 21 DIV for experiments. Whole cell recordings were made at −70 mV holding potential using Axopatch 200B and Clampex 8.0 software (Molecular Devices), filtering at 2 kHz and sampling at 5 kHz. The cells were visualized using a Zeiss Axiovert S100 microscope. The internal pipette solution contained 115mM $CsMeSO_3$, 10mM CsCl, 5mM NaCl, 10mM HEPES, 0.6 mM EGTA, 20mM tetraethylammonium chloride, 4mM Mg-ATP, 0.3mM Na_2GTP and 10mM QX-314 (lidocaine N-ethyl bromide). The final solution was adjusted to pH 7.35 and 300 mOsm. Final resistance of the electrode tips was ~ 3–6 MΩ. For all experiments, the extracellular solution was a modified Tyrode's solution containing 150mM NaCl, 4mM KCl, 10mM glucose, 10mM HEPES, 2mM $MgCl_2$ and 2mM $CaCl_2$, adjusted to pH 7.4 and 310 mOsm. To isolate IPSCs, postsynaptic ionotropic glutamate receptors antagonists 6-cyano-7-nitroquinoxaline-2,3-dione (CNQX; Sigma) and aminophosphonopentanoic acid (AP-5; Sigma) were added at concentrations of 10 μM and 50 μM, respectively. To elicit evoked responses, electrical stimulation was delivered through parallel platinum electrodes with a constant current unit (WPI A385) set at 30 mA. Spontaneous mIPSCs were recorded with the addition of 1 μM TTX. mIPSC events were identified with a 4-pA detection threshold and analyzed with MiniAnalysis.

Fluorescence Imaging

Experimental set up and stimulation protocol: 16–21 DIV cultured pyramidal neurons expressing vGlut1-pHluorin were used for the imaging experiments. The modified Tyrode's solution from above containing 2, 4, 8 mM Ca^{2+} or Sr^{2+} was used with 10 μM CNQX and 50 μM AP-5 to prevent recurrent network activity. Experiments were performed at room temperature using an Andor iXon+ back-illuminated EMCCD camera (Model no. DU-897E-CSO-#BV) collected on a Nikon Eclipse TE2000-U microscope with a 100X Plan Fluor objective (Nikon). For illumination we used a Lambda-DG4 (Sutter instruments) with a FITC filter. Images were acquired at ~7 Hz with an exposure time of 120 ms and binning of 4 by 4 to optimize the signal-to-noise ratio. Neurons were stimulated using parallel bipolar electrodes (FHC) delivering 30 mA pulses at 10, 30, 40, 60s intervals, followed by a rest period prior to 100 APs delivered at 20 Hz. Data was collected using Nikon Elements Ar software, 3 μm square regions of interest (ROIs) and the resulting fluorescence values were exported to Microsoft Excel for analysis.

Surface and internal distribution assessment: To calculate surface versus intracellular distribution of syt7-pHluorin, we perfused a modified Tyrode's solution at pH=5.5 (buffered by MES instead of HEPES) to quench surface pHluorin and recorded for 30 s. After imaging putative boutons for another 30 s, a modified Tyrode's solution containing 20 mM NH4Cl was perfused for 30 s, in order to alkalinize all compartments. The difference of the mean fluorescence during acid buffer perfusion and normal Tyrode's solution correspond to the surface pool of pHluorin, while the difference in mean fluorescence between NH4Cl perfusion and normal Tyrode's solution correspond to the internal pool of pHluorin.

Fluorescence analysis: Fluorescence intensity traces were analyzed using Microsoft Excel and a custom made Matlab script, based on our previous analysis with some modifications (Leitz and Kavalali, 2011). Photobleaching was corrected with an exponential decay and

Author Manuscript Author Manuscript Author Manuscript Author Manuscript

background was subtracted linearly, both photobleaching and background values were calculated based on fluorescence measurements of background in each imaging experiment and also for each ROI. For single-vesicle analysis, successful fusion events were those that meet the following restrictions: event fluorescence amplitude must be greater than twice the standard deviation of the baseline (average of ~2.5 s prior to the event) and smaller than the mean single event amplitude plus two standard deviations (to select single vesicle fusion events, this value was determined experimentally in the lab using control cultures in 2 mM Ca^{2+} and checked regularly), and event time has to be coincident with the time of stimulation. Dwell times were calculated as the time between the initial fluorescence step and the start of fluorescence decay predicted by the best fit decay (using a goodness of fit parameter).Decay time constants were determined by fitting data with single exponential decay curves using Levenberg-Marquardt least sum of squares minimizations (a minimum of 10 points, ~1.7s, was required for the fitting after calculating dwell times). For 20 Hz stimulation, amplitude measurement and single exponential decay fitting was also performed in an automatized way using Matlab.

QUANTIFICATION AND STATISTICAL ANALYSIS

For imaging experiments, n refers to the number of experiments performed with each experiment containing up to 50 regions of interest. Statistical analysis was performed on GraphPad Prism software. Student's t-test (2-tailed, unpaired) was used to analyze all pairwise data sets obtained from synapses under distinct conditions. The Kolmogorov–Smirnov (K-S) test was used to determine differences in cumulative probability histograms when comparing 2 groups, for 3 or more groups histograms were compared using Kruskal-Wallis test and Dunn's multiple comparison post-test. For parametric analysis of multiple comparisons, two-way ANOVA and one-way ANOVA with Bonferroni or Tukey post hoc analysis were used. Number of experiments and other relevant statistical information is provided on the corresponding figure legends. In general, mean ± SEM is informed and plotted, unless stated otherwise. A statistical significant difference between groups was reached when $p \leq 0.05$ was reached (specific p values are provided in the legends to the figures).

Supplementary Material

Refer to Web version on PubMed Central for supplementary material.

Acknowledgments

We are grateful to Brent Trauterman for his technical assistance. We would like to thank Drs. Helmut Kramer, and Jose Rizo-Rey for their critical comments on the manuscript. This work was supported by a grant from the National Institute of Mental Health (MH066198).

References

Bacaj T, Wu D, Yang X, Morishita W, Zhou P, Xu W, Malenka RC, Sudhof TC. Synaptotagmin-1 and synaptotagmin-7 trigger synchronous and asynchronous phases of neurotransmitter release. Neuron. 2013; 80:947–959. [PubMed: 24267651]

Author Manuscript Author Manuscript Author Manuscript Author Manuscript

Bal M, Leitz J, Reese AL, Ramirez DM, Durakoglugil M, Herz J, Monteggia LM, Kavalali ET. Reelin mobilizes a VAMP7-dependent synaptic vesicle pool and selectively augments spontaneous neurotransmission. Neuron. 2013; 80:934–946. [PubMed: 24210904]

Balaji J, Ryan TA. Single-vesicle imaging reveals that synaptic vesicle exocytosis and endocytosis are coupled by a single stochastic mode. Proc Natl Acad Sci U S A. 2007; 104:20576–20581. [PubMed: 18077369]

Bronk P, Deak F, Wilson MC, Liu XR, Sudhof TC, Kavalali ET. Differential effects of SNAP-25 deletion on Ca2+-dependent and Ca2+-independent neurotransmission. J Neurophysiol. 2007; 98:794–806. [PubMed: 17553942]

Deak F, Schoch S, Liu X, Sudhof TC, Kavalali ET. Synaptobrevin is essential for fast synaptic-vesicle endocytosis. Nat Cell Biol. 2004; 6:1102–1108. [PubMed: 15475946]

Dean C, Dunning FM, Liu H, Bomba-Warczak E, Martens H, Bharat V, Ahmed S, Chapman ER. Axonal and dendritic synaptotagmin isoforms revealed by a pHluorin-syt functional screen. Mol Biol Cell. 2012; 23:1715–1727. [PubMed: 22398727]

Dodge FA Jr, Miledi R, Rahamimoff R. Strontium and quantal release of transmitter at the neuromuscular junction. J Physiol. 1969; 200:267–283. [PubMed: 4387376]

Evans CS, Ruhl DA, Chapman ER. An Engineered Metal Sensor Tunes the Kinetics of Synaptic Transmission. Journal of Neuroscience. 2015; 35:11769–11779. [PubMed: 26311762]

Fernandez-Alfonso T, Ryan TA. A heterogeneous “resting” pool of synaptic vesicles that is dynamically interchanged across boutons in mammalian CNS synapses. Brain Cell Biol. 2008; 36:87–100. [PubMed: 18941900]

Fernandez-Chacon R, Konigstorfer A, Gerber SH, Garcia J, Matos MF, Stevens CF, Brose N, Rizo J, Rosenmund C, Sudhof TC. Synaptotagmin I functions as a calcium regulator of release probability. Nature. 2001; 410:41–49. [PubMed: 11242035]

Geppert M, Goda Y, Hammer RE, Li C, Rosahl TW, Stevens CF, Sudhof TC. Synaptotagmin I: a major Ca2+ sensor for transmitter release at a central synapse. Cell. 1994; 79:717–727. [PubMed: 7954835]

Haucke V, De Camilli P. AP-2 recruitment to synaptotagmin stimulated by tyrosine-based endocytic motifs. Science. 1999; 285:1268–1271. [PubMed: 10455054]

Hosoi N, Holt M, Sakaba T. Calcium dependence of exo- and endocytotic coupling at a glutamatergic synapse. Neuron. 2009; 63:216–229. [PubMed: 19640480]

Hosoi N, Sakaba T, Neher E. Quantitative analysis of calcium-dependent vesicle recruitment and its functional role at the calyx of held synapse. Journal of Neuroscience. 2007; 27:14286–14298. [PubMed: 18160636]

Jackman SL, Turecek J, Belinsky JE, Regehr WG. The calcium sensor synaptotagmin 7 is required for synaptic facilitation. Nature. 2016; 529:88–91. [PubMed: 26738595]

Kavalali ET. Synaptic vesicle reuse and its implications. Neuroscientist. 2006; 12:57–66. [PubMed: 16394193]

Kavalali ET, Jorgensen EM. Visualizing presynaptic function. Nat Neurosci. 2014; 17:10–16. [PubMed: 24369372]

Kononenko NL, Haucke V. Molecular mechanisms of presynaptic membrane retrieval and synaptic vesicle reformation. Neuron. 2015; 85:484–496. [PubMed: 25654254]

Lee J, Guan Z, Akbergenova Y, Littleton JT. Genetic analysis of synaptotagmin C2 domain specificity in regulating spontaneous and evoked neurotransmitter release. J Neurosci. 2013; 33:187–200. [PubMed: 23283333]

Leitz J, Kavalali ET. Ca(2)(+) influx slows single synaptic vesicle endocytosis. J Neurosci. 2011; 31:16318–16326. [PubMed: 22072683]

Leitz J, Kavalali ET. Fast retrieval and autonomous regulation of single spontaneously recycling synaptic vesicles. Elife. 2014; 3:e03658. [PubMed: 25415052]

Leitz J, Kavalali ET. Ca2+ Dependence of Synaptic Vesicle Endocytosis. Neuroscientist. 2015

Luo F, Bacaj T, Sudhof TC. Synaptotagmin-7 Is Essential for Ca2+-Triggered Delayed Asynchronous Release But Not for Ca2+-Dependent Vesicle Priming in Retinal Ribbon Synapses. J Neurosci. 2015; 35:11024–11033. [PubMed: 26245964]

Author Manuscript Author Manuscript Author Manuscript Author Manuscript

Marks B, McMahon HT. Calcium triggers calcineurin-dependent synaptic vesicle recycling in mammalian nerve terminals. Curr Biol. 1998; 8:740–749. [PubMed: 9651678]

Maximov A, Lao Y, Li H, Chen X, Rizo J, Sorensen JB, Sudhof TC. Genetic analysis of synaptotagmin-7 function in synaptic vesicle exocytosis. Proc Natl Acad Sci U S A. 2008; 105:3986–3991. [PubMed: 18308933]

Maximov A, Sudhof TC. Autonomous function of synaptotagmin 1 in triggering synchronous release independent of asynchronous release. Neuron. 2005; 48:547–554. [PubMed: 16301172]

Maximov A, Tang J, Yang X, Pang ZP, Sudhof TC. Complexin controls the force transfer from SNARE complexes to membranes in fusion. Science. 2009; 323:516–521. [PubMed: 19164751]

McMahon HT, Missler M, Li C, Sudhof TC. Complexins: cytosolic proteins that regulate SNAP receptor function. Cell. 1995; 83:111–119. [PubMed: 7553862]

Mozhayeva MG, Sara Y, Liu X, Kavalali ET. Development of vesicle pools during maturation of hippocampal synapses. J Neurosci. 2002; 22:654–665. [PubMed: 11826095]

Murthy VN, Sejnowski TJ, Stevens CF. Heterogeneous release properties of visualized individual hippocampal synapses. Neuron. 1997; 18:599–612. [PubMed: 9136769]

Nicholson-Fish JC, Kokotos AC, Gillingwater TH, Smillie KJ, Cousin MA. VAMP4 Is an Essential Cargo Molecule for Activity-Dependent Bulk Endocytosis. Neuron. 2015:88. [PubMed: 25569348]

Nicholson-Tomishima K, Ryan TA. Kinetic efficiency of endocytosis at mammalian CNS synapses requires synaptotagmin I. Proc Natl Acad Sci U S A. 2004; 101:16648–16652. [PubMed: 15492212]

Poskanzer KE, Fetter RD, Davis GW. Discrete residues in the c(2)b domain of synaptotagmin I independently specify endocytic rate and synaptic vesicle size. Neuron. 2006; 50:49–62. [PubMed: 16600855]

Poskanzer KE, Marek KW, Sweeney ST, Davis GW. Synaptotagmin I is necessary for compensatory synaptic vesicle endocytosis in vivo. Nature. 2003; 426:559–563. [PubMed: 14634669]

Raingo J, Khvotchev M, Liu P, Darios F, Li YC, Ramirez DM, Adachi M, Lemieux P, Toth K, Davletov B, Kavalali ET. VAMP4 directs synaptic vesicles to a pool that selectively maintains asynchronous neurotransmission. Nat Neurosci. 2012; 15:738–745. [PubMed: 22406549]

Reim K, Mansour M, Varoqueaux F, McMahon HT, Sudhof TC, Brose N, Rosenmund C. Complexins regulate a late step in Ca2+-dependent neurotransmitter release. Cell. 2001; 104:71–81. [PubMed: 11163241]

Rizo J, Rosenmund C. Synaptic vesicle fusion. Nat Struct Mol Biol. 2008; 15:665–674. [PubMed: 18618940]

Sankaranarayanan S, Ryan TA. Real-time measurements of vesicle-SNARE recycling in synapses of the central nervous system. Nat Cell Biol. 2000; 2:197–204. [PubMed: 10783237]

Shin OH, Rhee JS, Tang J, Sugita S, Rosenmund C, Sudhof TC. Sr2+ binding to the Ca2+ binding site of the synaptotagmin 1 C2B domain triggers fast exocytosis without stimulating SNARE interactions. Neuron. 2003; 37:99–108. [PubMed: 12526776]

Sudhof TC. The synaptic vesicle cycle. Annu Rev Neurosci. 2004; 27:509–547. [PubMed: 15217342]

Sudhof TC. Calcium control of neurotransmitter release. Cold Spring Harb Perspect Biol. 2012; 4:a011353. [PubMed: 22068972]

Sudhof TC. Neurotransmitter Release: The Last Millisecond in the Life of a Synaptic Vesicle. Neuron. 2013; 80:675–690. [PubMed: 24183019]

Sugita S, Shin OH, Han WP, Lao Y, Sudhof TC. Synaptotagmins form a hierarchy of exocytotic Ca2+ sensors with distinct Ca2+ affinities. Embo J. 2002; 21:270–280. [PubMed: 11823420]

Takamori S, Holt M, Stenius K, Lemke EA, Gronborg M, Riedel D, Urlaub H, Schenck S, Brugger B, Ringler P, et al. Molecular anatomy of a trafficking organelle. Cell. 2006; 127:831–846. [PubMed: 17110340]

Tang J, Maximov A, Shin OH, Dai H, Rizo J, Sudhof TC. A complexin/synaptotagmin 1 switch controls fast synaptic vesicle exocytosis. Cell. 2006; 126:1175–1187. [PubMed: 16990140]

Virmani T, Han W, Liu X, Sudhof TC, Kavalali ET. Synaptotagmin 7 splice variants differentially regulate synaptic vesicle recycling. Embo J. 2003; 22:5347–5357. [PubMed: 14532108]

Author Manuscript Author Manuscript Author Manuscript Author Manuscript

Voglmaier SM, Kam K, Yang H, Fortin DL, Hua ZL, Nicoll RA, Edwards RH. Distinct endocytic pathways control the rate and extent of synaptic vesicle protein recycling. Neuron. 2006; 51:71–84. [PubMed: 16815333]

von Gersdorff H, Matthews G. Inhibition of endocytosis by elevated internal calcium in a synaptic terminal. Nature. 1994; 370:652–655. [PubMed: 8065451]

von Poser C, Zhang JZ, Mineo C, Ding W, Ying Y, Sudhof TC, Anderson RG. Synaptotagmin regulation of coated pit assembly. J Biol Chem. 2000; 275:30916–30924. [PubMed: 10906143]

Weber JP, Toft-Bertelsen TL, Mohrmann R, Delgado-Martinez I, Sorensen JB. Synaptotagmin-7 is an asynchronous calcium sensor for synaptic transmission in neurons expressing SNAP-23. PLoS One. 2014; 9:e114033. [PubMed: 25422940]

Wen H, Linhoff MW, McGinley MJ, Li GL, Corson GM, Mandel G, Brehm P. Distinct roles for two synaptotagmin isoforms in synchronous and asynchronous transmitter release at zebrafish neuromuscular junction. Proc Natl Acad Sci U S A. 2010; 107:13906–13911. [PubMed: 20643933]

Wu LG, Hamid E, Shin W, Chiang HC. Exocytosis and Endocytosis: Modes, Functions, and Coupling Mechanisms. Annu Rev Physiol. 2014; 76:301–331. [PubMed: 24274740]

Wu XS, McNeil BD, Xu J, Fan J, Xue L, Melicoff E, Adachi R, Bai L, Wu LG. Ca(2+) and calmodulin initiate all forms of endocytosis during depolarization at a nerve terminal. Nat Neurosci. 2009; 12:1003–1010. [PubMed: 19633667]

Xu-Friedman MA, Regehr WG. Probing fundamental aspects of synaptic transmission with strontium. J Neurosci. 2000; 20:4414–4422. [PubMed: 10844010]

Xu JH, Luo FJ, Zhang Z, Xue L, Wu XS, Chiang HC, Shin W, Wu LG. SNARE Proteins Synaptobrevin, SNAP-25, and Syntaxin Are Involved in Rapid and Slow Endocytosis at Synapses. Cell Rep. 2013; 3:1414–1421. [PubMed: 23643538]

Xu W, Morishita W, Buckmaster PS, Pang ZP, Malenka RC, Sudhof TC. Distinct Neuronal Coding Schemes in Memory Revealed by Selective Erasure of Fast Synchronous Synaptic Transmission. Neuron. 2012; 73:990–1001. [PubMed: 22405208]

Yang XF, Cao P, Sudhof TC. Deconstructing complexin function in activating and clamping Ca2+-triggered exocytosis by comparing knockout and knockdown phenotypes. Proc Natl Acad Sci U S A. 2013; 110:20777–20782. [PubMed: 24297916]

Yao J, Kwon SE, Gaffaney JD, Dunning FM, Chapman ER. Uncoupling the roles of synaptotagmin I during endo- and exocytosis of synaptic vesicles. Nat Neurosci. 2012a; 15:243–249.

Yao LH, Rao Y, Varga K, Wang CY, Xiao P, Lindau M, Gong LW. Synaptotagmin 1 is necessary for the Ca2+ dependence of clathrin-mediated endocytosis. J Neurosci. 2012b; 32:3778–3785. [PubMed: 22423098]

Zhang JZ, Davletov BA, Sudhof TC, Anderson RG. Synaptotagmin I is a high affinity receptor for clathrin AP-2: implications for membrane recycling. Cell. 1994; 78:751–760. [PubMed: 8087843]

Author Manuscript Author Manuscript Author Manuscript Author Manuscript

Highlights

- Loss of syt1, complexins or Sr^{2+} substitution slows endocytosis after activity
- Asynchronously released synaptic vesicles are retrieved via slow endocytosis
- Link between asynchronous release and slowed endocytosis requires synaptotagmin7
- Whereas, after synchronous single synaptic vesicle fusion, syt1 delays endocytosis

Author Manuscript Author Manuscript Author Manuscript Author Manuscript

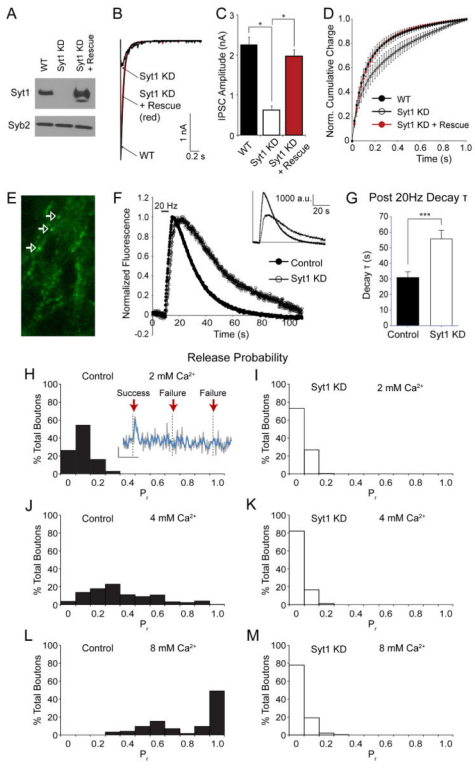

Figure 1. Syt1 knockdown slows multivesicle retrieval after repetitive stimulation

(A) Representative immunoblot showing decreased syt1 protein levels in neurons infected with syt1 KD lentivirus and sytin neurons co-infected with syt1 KD and shRNA-resistant syt1 expressing lentivirus. The expression of synaptobrevin 2 served as an endogenous control.

(B) Representative traces of IPSCs recordings evoked by single-pulse stimuli from WT neurons and neurons infected with lentivirus expressing syt1 shRNA (syt1 KD) and syt1 KD with shRNA-resistant syt1 (syt1 KD + Rescue).

(C) Peak amplitudes of single-stimulus evoked IPSCs in WT (n=17), syt1 KD (n=17) and syt1 KD rescue (n=14) neurons. Error bars in this and in all other figures indicate SEM and asterisks (*) denote statistical significance. Statistical significance was assessed using one-way ANOVA with Bonferroni correction ($p<0.000001$ for both conditions compared to syt1 KD). See Figure S1 for spontaneous IPSC events.

(D) Normalized cumulative IPSC charge for 1 s after the stimulus reveals slower peak latency in syt1 KD neurons consistent with previous experiments from syt1 knockout neurons. Two-way ANOVA without replication shows significant differences between the groups ($p<0.0001$).

(E) Example frame showing numerous punctate boutons (white arrows) in neurons infected with lentivirus expressing vGlut1-pHluorin.

(F) Average fluorescence traces of vGlut1-pHluorin in control and syt1 KD neurons in response to 20Hz stimulation for 5s. Inset, non-normalized fluorescence traces.

(G) Average decay time constants (τ) of the fluorescence return to baseline after 20 Hz stimulation in control (n=989 boutons from 11 coverslips) and syt1 KD neurons (n= 508 boutons from 8 coverslips). Syt1 KD post-20Hz decay τ was significantly greater than

Author Manuscript Author Manuscript Author Manuscript Author Manuscript

control ($p<0.001$) assessed by one-way ANOVA with Tukey's multiple comparisons post-test.

(H) Histogram of release probability distribution by bouton for control neurons in response to low frequency single-AP stimuli in 2 mM extracellular Ca^{2+}. Inset, example trace showing a successful event and two failures where the dotted lines indicate when stimuli were applied. The raw fluorescence trace is in gray with a moving average of 4 points (~0.5 s) depicted by the blue line. Vertical scale bar represents 200 a.u. while horizontal scale bar is 5 s.

(I) Release probability distribution for syt1 KD neurons in 2 mM extracellular Ca^{2+}.

(J) Release probability distribution for control neurons in 4 mM extracellular Ca^{2+}.

(K) Release probability distribution for syt1 KD neurons in 4 mM extracellular Ca^{2+}.

(L) Release probability distribution for control neurons in 8 mM extracellular Ca^{2+}.

(M) Release probability distribution for syt1 KD neurons in 8 mM extracellular Ca^{2+}.

Author Manuscript Author Manuscript Author Manuscript Author Manuscript

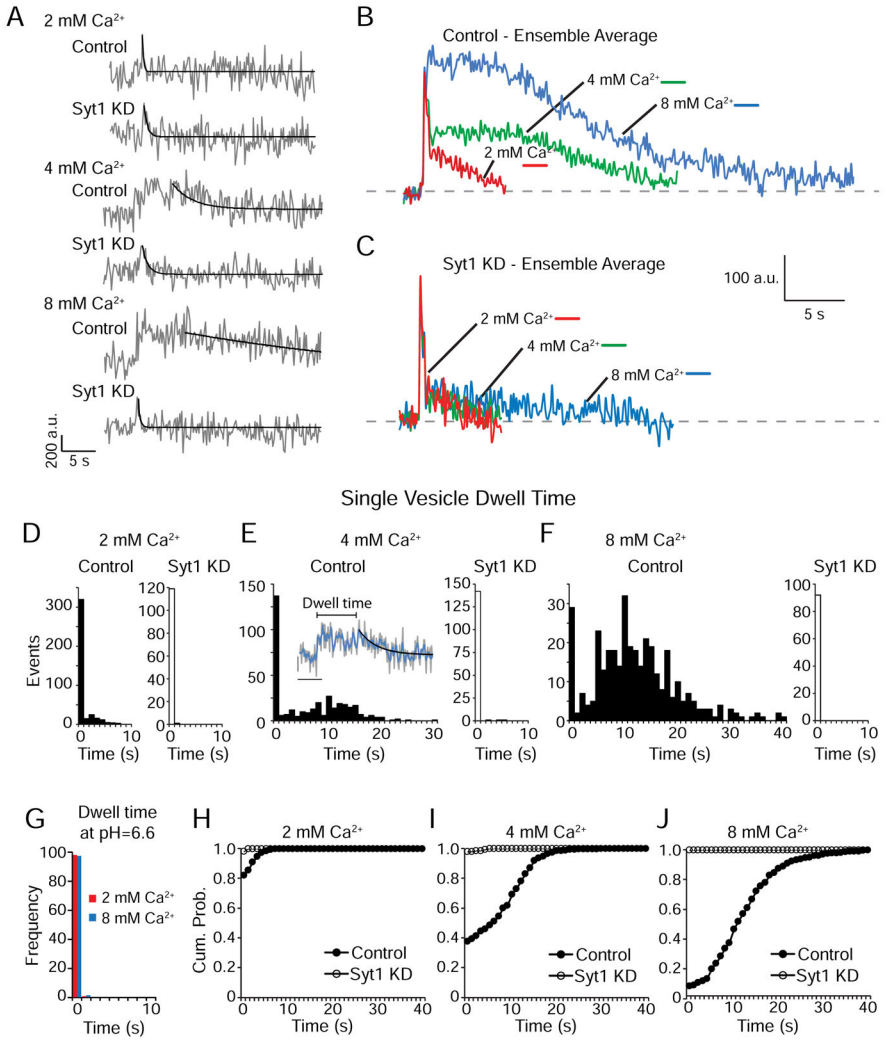

Figure 2. Syt1 KD accelerates retrieval of single-vesicle fusion events

(A) Sample traces of single-vesicle events observed in control and syt1 KD neurons in 2, 4 and 8 mM extracellular Ca^{2+}. The gray trace shows raw fluorescence data and the black trace is a single-exponential decay fit.

(B) Average non-normalized traces of single-vesicle events in control neurons in 2, 4 and 8 mM extracellular Ca^{2+}.

(C) Average non-normalized traces of single-vesicle events in syt1 KD neurons in 2, 4 and 8 mM extracellular Ca^{2+}.

(D) Distribution of single-vesicle dwell times from control (left, n=473 events from 7 coverslips) and syt1 KD (right, n=120 events from 8 coverslips) neurons in 2 mM extracellular Ca^{2+}.

(E) Distribution of single-vesicle dwell times from control (left, n=365 events from 6 coverslips) and syt1 KD (right, n=145 events from 18 coverslips) neurons in 4 mM extracellular Ca^{2+}. Inset, example trace showing an event with dwell time marked and a single-exponential fit curve (black) for decay τ calculation (see Figure S2). The raw

Author Manuscript Author Manuscript Author Manuscript Author Manuscript

fluorescence trace is in gray with a moving average of 4 points (~0.5 s) depicted by the blue line. Vertical scale bar represents 200 a.u. while horizontal scale bar is 5 s.

(F) Distribution of single-vesicle dwell times from control (left, n=356 events from 10 coverslips) and syt1 KD (right, n=124 events from 14 coverslips) neurons in 8 mM extracellular Ca^{2+}.

(G) Distribution of single-vesicle dwell times from control neurons at 2 and 8 mM Ca^{2+} (131 boutons from 2 coverslips and 215 boutons from 3 coverslips respectively) under perfusion of a pH=6.6 buffer, showing the absence of dwell times when surface fluorescence is quenched.

(H) Cumulative probability histograms of dwell times from control and syt1 KD neurons in 2 mM extracellular Ca^{2+} are significantly different ($p<0.05$) according to the K-S test.

(I) Cumulative probability histograms of dwell times from control and syt1 KD neurons in 4 mM extracellular Ca^{2+} are significantly different ($p< 0.0001$) according to the K-S test.

(J) Cumulative probability histograms of dwell times from control and syt1 KD neurons in 8 mM extracellular Ca^{2+} are significantly different ($p< 0.0001$) according to the K-S test.

Author Manuscript Author Manuscript Author Manuscript Author Manuscript

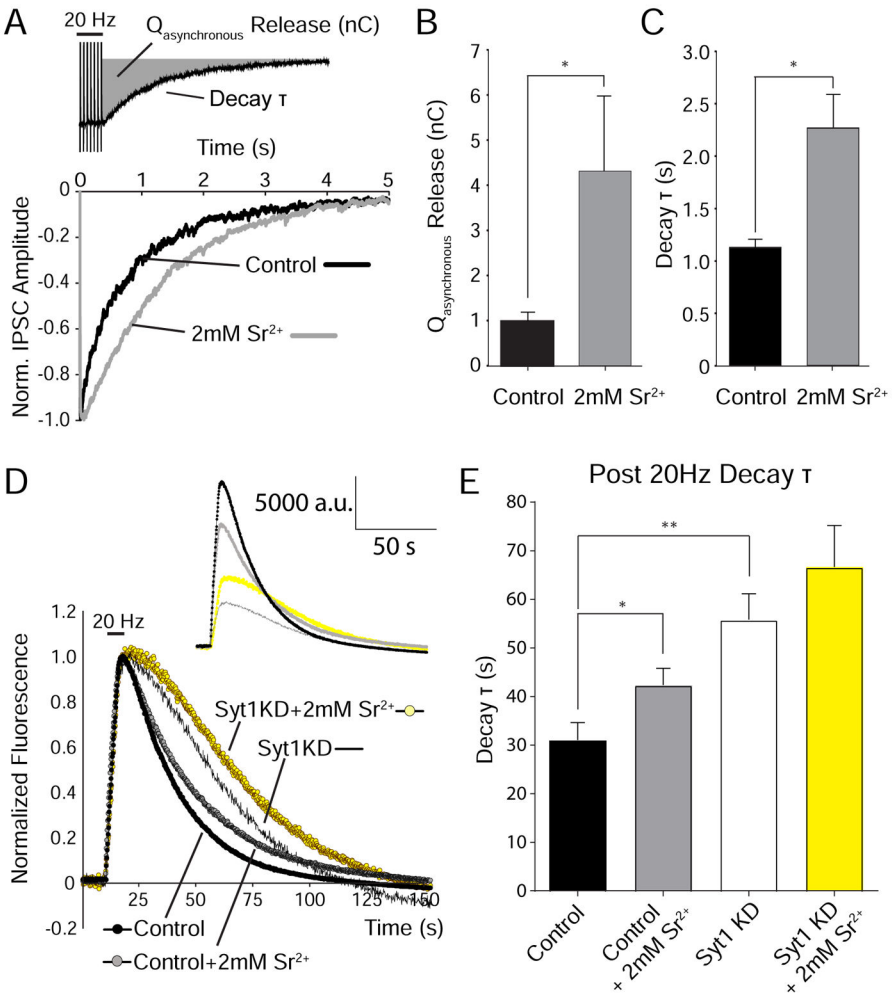

Figure 3. Sr^{2+} promotes asynchronous release and slows vesicle retrieval after 20 Hz stimulation

(A) Top, schematic depicting the experimental paradigm and two measures of asynchronous release after 100 APs at 20 Hz. Total asynchronous release charge ($Q_{asynchronous}$ release) was calculated as the area from the onset of the final stimulation to the baseline (gray area). Decay τ from a single-exponential fit quantified the time course of the return to baseline. Bottom, sample IPSC traces for 5 s after the final stimulation in 2 mM Ca^{2+} and 2 mM Sr^{2+}.

(B) Average $Q_{asynchronous}$ release was significantly increased in 2 mM Sr^{2+} (n=5) compared to 2 mM Ca^{2+} control (n=10) ($p<0.05$).

(C) Average decay τ of IPSCs back to baseline is significantly increased in 2 mM Sr^{2+} compared to 2 mM Ca^{2+} control ($p<0.0005$).

(D) Average fluorescence traces of vGlut1-pHluorin in control and syt1 KD groups, in the presence of either extracellular 2 mM Ca^{2+} or 2 mM Sr^{2+}, in response to 20Hz stimulation for 5s. Inset, non-normalized fluorescence traces.

(E) Average decay τ for each group, Sr^{2+} significantly slows down multi-vesicular endocytosis in control group but not in syt1 KD (control vs control + Sr^{2+} $p<0.05$; control vs syt1 KD $p<0.003$; assessed by one-way ANOVA with Tukey's multiple comparisons post-test). Control: 989 boutons from 11 coverslips; Control + Sr^{2+}: 551 boutons from 8

Author Manuscript Author Manuscript Author Manuscript Author Manuscript

coverslips; syt1 KD: 508 boutons from 8 coverslips; syt1 KD + Sr^{2+}: 262 boutons from 5 coverslips. Mean values per coverslip were compared.

Author Manuscript Author Manuscript Author Manuscript Author Manuscript

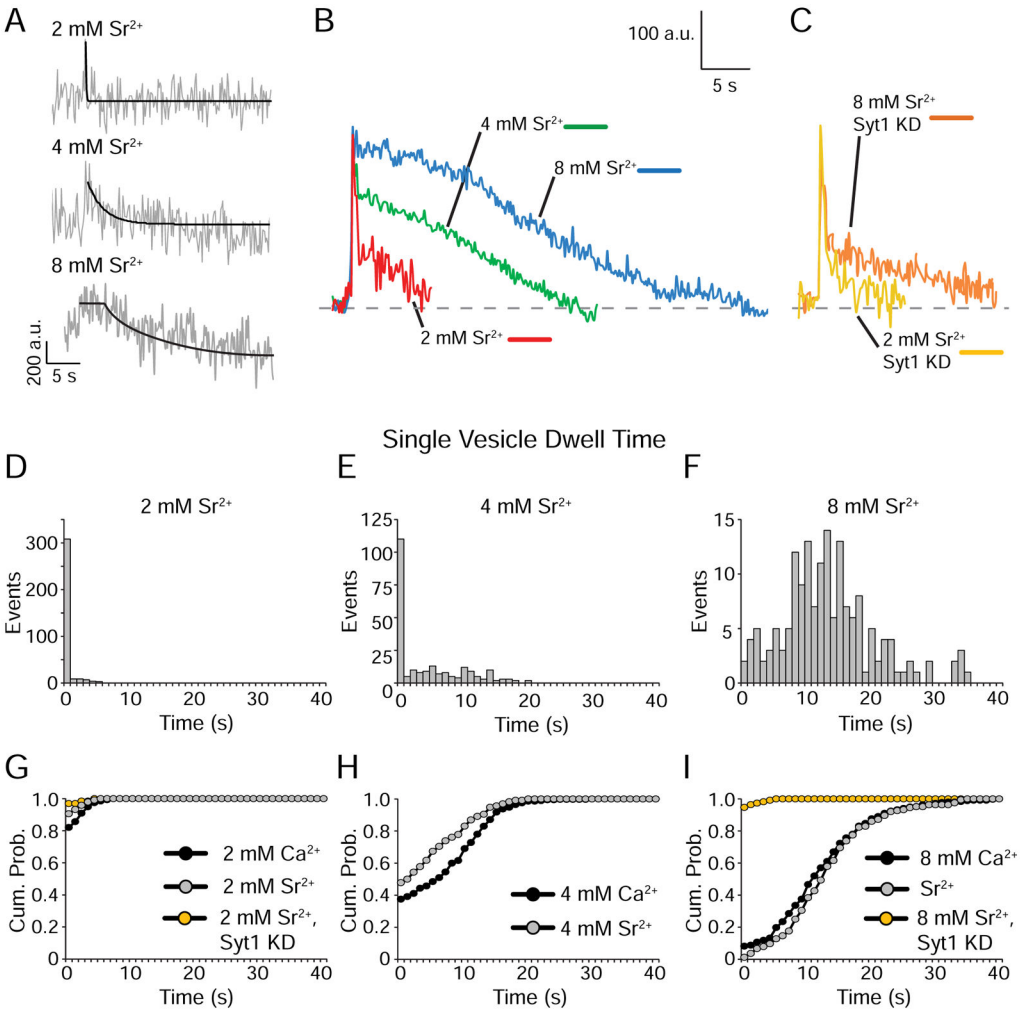

Figure 4. Sr^{2+} can substitute for Ca^{2+} in regulation of single-vesicle retrieval kinetics

(A) Sample traces of single-vesicle events observed in neurons in 2, 4 and 8 mM Sr^{2+}. The gray trace shows raw fluorescence data and the black trace is a single-exponential decay fit.

(B) Average non-normalized traces of single-vesicle events from neurons in 2, 4, and 8 mM extracellular Sr^{2+}.

(C) Average non-normalized traces of single-vesicle events from syt1 KD neurons in 2 and 8 mM extracellular Sr^{2+}.

(D) Distribution of single-vesicle dwell times from neurons in 2 mM extracellular Sr^{2+} (n=340 events from 6 coverslips).

(E) Distribution of single-vesicle dwell times from neurons in 4 mM extracellular Sr^{2+} (n=230 events from 5 coverslips).

(F) Distribution of single-vesicle dwell times from neurons in 8 mM extracellular Sr^{2+} (n=164 events from 5 coverslips).

(G) Cumulative probability histograms of single-vesicle dwell times for neurons in 2 mM Ca^{2+} and 2 mM Sr^{2+} and syt1 neurons in 2 mM Sr^{2+} (n=65 events from 6 coverslips). No significant difference between conditions according to the K-S test.

Author Manuscript Author Manuscript Author Manuscript Author Manuscript

(H) Cumulative probability histograms of single-vesicle dwell times for neurons in 4 mM Ca^{2+} and 4 mM Sr^{2+} show a significant difference ($p<0.0001$) according to the K-S test. (I) Cumulative probability histograms of single-vesicle dwell times for neurons in 8 mM Ca^{2+} and 8 mM Sr^{2+} and syt1 KD neurons in 8 mM Sr^{2+} (n=112 events from 6 coverslips). K-S tests show no significant difference between dwell times in 8 mM Ca^{2+} and 8 mM Sr^{2+} but dwell times in 8 mM Sr^{2+} in syt1 KD neurons were significantly different from both other conditions ($p<0.0001$). See also Figure S3.

Author Manuscript Author Manuscript Author Manuscript Author Manuscript

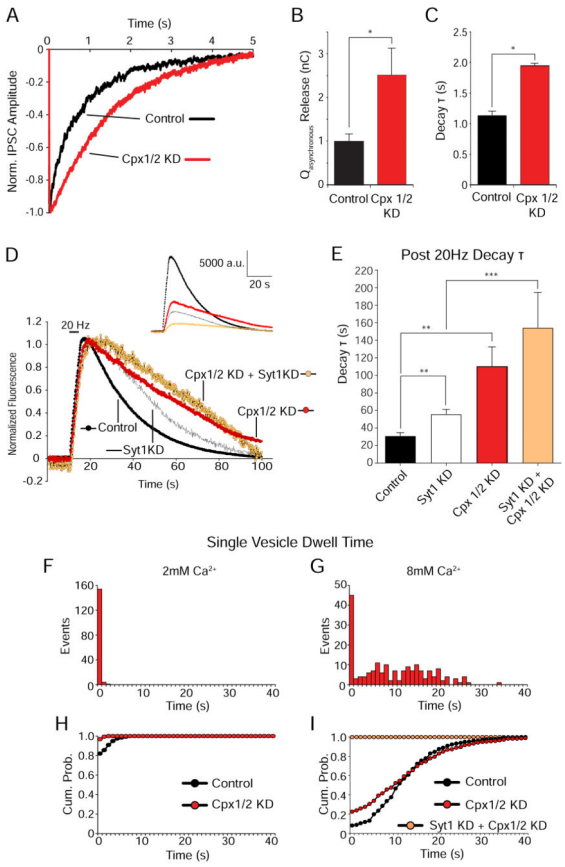

Figure 5. Cpx1/2 KD slows vesicle retrieval after 20 Hz stimulation but minimally affect single-vesicle retrieval time

(A) Sample IPSC traces for 5 s after the final stimulation in control and Cpx1/2 KD neurons (same experimental paradigm and analysis as explained in Figure 3A).

(B) Average $Q_{asynchronous}$ release was significantly increased in Cpx1/2 KD neurons (n=7) compared to WT control (n=10) ($p<0.05$).

(C) Average decay **τ** of IPSCs back to baseline is significantly increased in Cpx1/2 KD compared to WT control ($p<0.05$).

(D) Average fluorescence traces of vGlut1-pHluorin in control and syt1 KD groups, with or without complexin 1 and 2 (Cpx1/2) KD co-expression, in response to 20Hz stimulation for 5s. Inset, non-normalized fluorescence traces.

(E) Average decay **τ**, elimination of Cpx1/2 drastically slows down endocytic rate in control and in syt1 KD groups (control vs syt1 KD $p<0.003$; control vs Cpx1/2 KD $p<0.003$; syt1 KD vs syt1 KD + Cpx1/2 KD $p<0.0004$; assessed by one-way ANOVA with Tukey's multiple comparisons post-test). Control: 989 boutons from 11 coverslips; syt1 KD: 508 boutons from 8 coverslips; Cpx1/2 KD: 800 boutons from 11 coverslips; syt1 KD + Cpx1/2 KD: 314 boutons from 7 coverslips. Mean values per coverslip were compared.

(F) Distribution of single-vesicle dwell times from Cpx1/2 KD neurons in 2 mM extracellular Ca^{2+} (n=159 events from 6 coverslips).

(G) Distribution of single-vesicle dwell times from Cpx1/2 KD neurons in 8 mM extracellular Ca^{2+} (n=185 events from 7 coverslips).

Author Manuscript Author Manuscript Author Manuscript Author Manuscript

(H) Cumulative probability histograms of single-vesicle dwell times for control and Cpx1/2 KD neurons in 2 mM Ca^{2+} show a significant difference ($p<0.05$) according to the K-S test. (I) Cumulative probability distribution of single-vesicle dwell times for control and Cpx1/2 KD neurons in 8 mM Ca^{2+} show a significant difference ($p<0.0001$) according to the K-S test. See also Figure S4.

Author Manuscript Author Manuscript Author Manuscript Author Manuscript

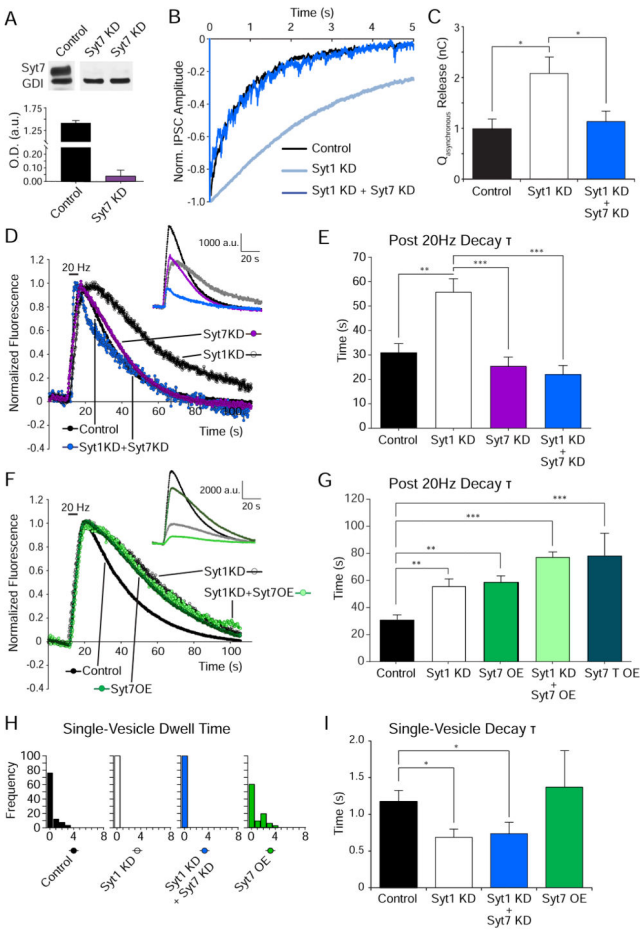

Figure 6. Syt7 KD reinstates faster synaptic multiple-vesicle retrieval in syt1 KD background

(A) Sample IPSC traces for 5 s after the final stimulation in control, syt1 KD and syt1 + syt7 DKD neurons (same experimental paradigm and analysis as explained in Figure 3A).

(B) Average $Q_{asynchronous}$ release for WT control (n=10), syt1 KD (n=8) and syt1 + syt7 DKD (n=8) neurons. One-way ANOVA with Bonferroni correction ($p<0.05$ for both conditions compared to syt1 KD) shows that syt7 KD rescues synchronous release in the syt1 KD background.

(C) Top, representative immunoblot showing decreased syt7 protein levels in neurons infected with syt7 KD lentivirus, GDI (Rab GDP dissociation inhibitor alpha) is a control. Bottom, quantification of syt7/GDI ratio in control and syt7 KD neurons (samples from 3 and 5 different cultures respectively).

(D) Average fluorescence traces of vGlut1-pHluorin in control, syt1 KD, syt7 KD and syt1+syt7 DKD neurons in response to 20Hz stimulation for 5s. Inset, non-normalized fluorescence traces.

(E) Average decay τ of the fluorescence return to baseline after 20 Hz stimulation in syt1 + syt7 DKD neurons is significantly decreased compared to syt1 KD neurons.

(F) Average fluorescence traces of vGlut1-pHluorin in control, syt1 KD, syt7 OE and syt1 KD + syt7 OE neurons in response to 20Hz stimulation for 5s. Inset, non-normalized fluorescence traces.

Author Manuscript Author Manuscript Author Manuscript Author Manuscript

(G) Average decay τ of the fluorescence return to baseline after 20 Hz stimulation in syt7 OE neurons is significantly increased compared to control, and addition of syt1 KD on syt7 OE neurons does not increase further the speed of endocytosis.

For D to G, control: 989 boutons from 11 coverslips; syt1 KD: 508 boutons from 8 coverslips; syt7 KD: N boutons from 8 coverslips; syt1 KD + syt7 KD: 393 boutons from 11 coverslips; syt7 OE: 96 boutons from 2 coverslips; syt1 KD + syt7 OE: 273 boutons from 4 coverslips; syt7 T OE: 292 boutons from 4 coverslips. Mean values per coverslip were compared by one-way ANOVA with Tukey's multiple comparisons post-test (** $p<0.003$; *** $p<0.001$).

(H) Top, distribution of single-vesicle dwell times from control (black), syt1 KD (white), syt1+syt7 DKD (blue) and syt7 OE (green) in 2 mM Ca^{2+}. Bottom, corresponding cumulative probability histograms. While control and syt7 OE neurons show a small proportion of events (~20–30 %) with dwell times after fusion, this is almost absent in syt1 KD and syt1 + syt7 DKD neurons.

(I) Average single-vesicle decay τ for control, syt1 KD, syt1+syt7 DKD, and syt7 OE neurons. One-way ANOVA with Bonferroni correction shows that events in syt1 KD and syt1 + syt7 DKD neurons decay faster than those in control and syt7 OE neurons ($p<0.005$).

Author Manuscript Author Manuscript Author Manuscript Author Manuscript

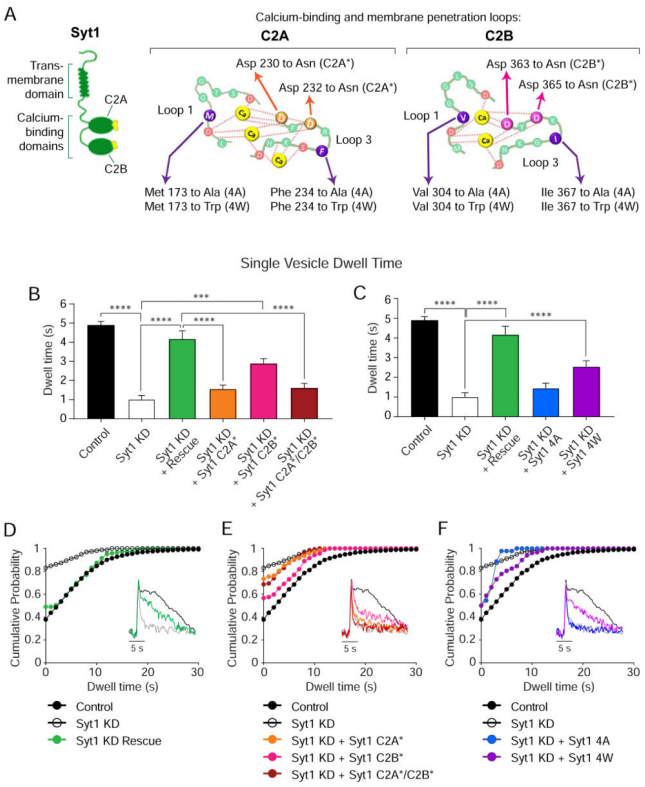

Figure 7. Ca^{2+}-binding and membrane penetration properties of syt1 are necessary to rescue single-vesicle retrieval kinetics after syt1 KD

(A) Left, schematic representation of syt1 and its domains. Right, amino acid sequence of the Ca^{2+}-binding loops of C2A and C2B domains, showing the position of the mutations studied.

(B) Multiple comparisons of mean dwell time values among control (black), syt1 KD (white) and Ca^{2+}-binding syt1 mutants, in 8 mM Ca^{2+}. syt1 that cannot bind Ca^{2+} through its C2B domain can only partially rescue (pink), compared to full length syt1 (green), while mutations in C2A (orange) or both C2A/C2B domains (dark red) render syt1 unable to rescue the phenotype.

(C) Multiple comparison of mean dwell time values among control (black), syt1 KD (white) and membrane penetration syt1 mutants, in 8 mM Ca^{2+}. syt1 that cannot penetrate membranes (syt1 4A, blue) is unable to rescue the phenotype, while a mutant with enhanced membrane penetration properties (syt1 4W, purple) can partially rescue compared to full length syt1 (green).

(D) Cumulative probability histograms of single-vesicle dwell times from control, syt1 KD and syt1 KD + rescue neurons, in 8 mM Ca^{2+}.

(E) Cumulative probability histograms of single-vesicle dwell times from control, syt1 KD, syt1 KD + syt1 C2A*, syt1 KD + syt1 C2B* and syt1 KD + syt1 C2A*/C2B* neurons, in 8 mM Ca^{2+}.

(F) Cumulative probability histograms of single-vesicle dwell times from control, syt1 KD, syt1 KD + syt1 4A and syt1 KD + syt1 4W neurons, in 2 8M Ca^{2+}.

Author Manuscript Author Manuscript Author Manuscript Author Manuscript

Control: 1241 events from 5 coverslips; syt1 KD: 190 events from 8 coverslips; syt1 KD + Rescue: 144 events from 5 coverslips; syt1 KD + syt1 C2A*: 215 events from 7 coverslips; syt1 KD + syt1 C2B*: 226 events from 7 coverslips; syt1 KD + syt1 C2A*/C2B*: 129 events from 6 coverslips; syt1 KD + syt1 4A: 44 events from 3 coverslips; syt1 KD + syt1 4W: 124 events from 5 coverslips. Non-parametric ANOVA analysis was performed applying Kruskal-Wallis test and Dunn's multiple comparison post-test (*** $p<0.0007$; **** $p<0.0001$).

Author Manuscript Author Manuscript Author Manuscript Author Manuscript

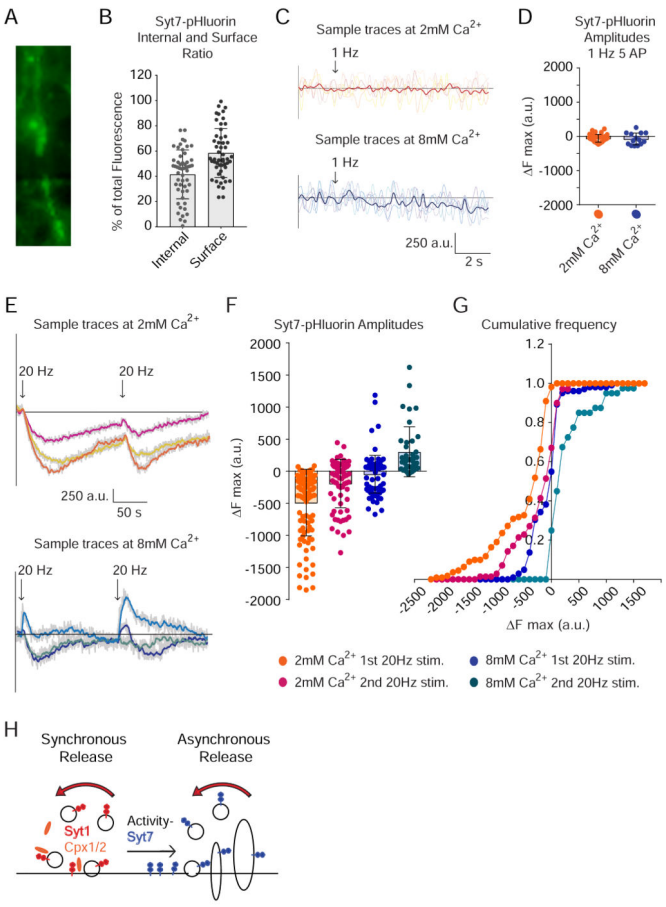

Figure 8. Syt7 is preferentially distributed to the presynaptic surface membrane and is endocytosed under strong stimulation

(A) Example image of syt7-pHluorin expression and fluorescence. Scale bar = 5 μm.

(B) Syt7-pHluorin distribution in internal and surface membranes, assessed by perfusion of Tyrode's buffer at pH=5.5 (data from 60 representative boutons).

(C) Sample fluorescence traces of syt7-pHluorin at 2 (top) and 8 (bottom) mM Ca^{2+} after 1 Hz stimulation for 5 s.

(D) Quantification of maximal fluorescence amplitude after 1 Hz stimulation shows no changes, i.e. no syt7-pHluorin trafficking after mild stimulation, either at 2 or 8 mM external Ca^{2+} (45 boutons from 4 coverslips).

(E) Sample fluorescence traces of syt7-pHluorin at 2 (top) and 8 (bottom) mM Ca^{2+} after two consecutive 20 Hz stimulations for 5 s.

(F) Quantification of maximal fluorescence amplitude after 20 Hz stimulation shows that syt7-pHluorin is primarily endocytosed (negative peak) at low Ca^{2+} levels, but at high Ca^{2+} levels and specially after an initial round ofstimulation, syt7-pHluorin is recycled and transported back to the plasma membrane (see individual ΔF_{max} values redistribute from negative towards positive values with increasing external Ca^{2+} concentration and/or the number of stimulations).

(G) Cumulative frequency histogram of the values presented in 8E. 1st stimulation at 20 Hz and 2 mM Ca^{2+}: 61 boutons from 5 coverslips; 2nd stimulation at 20 Hz and 2 mM Ca^{2+}: 21

Author Manuscript Author Manuscript Author Manuscript Author Manuscript

boutons from 2 coverslips; 1st stimulation at 20 Hz and 8 mM Ca^{2+}: 86 boutons from 5 coverslips; 2nd stimulation at 20 Hz and 8 mM Ca^{2+}: 24 boutons from 2 coverslips. (H) A model emerging from our results suggests that syt1 and complexin-dependent synchronous release is associated with rapid synaptic vesicle recycling pathways. In contrast, promoting asynchronous release targets synaptic vesicles towards slower recycling pathways in a syt7-dependent manner.